Automated fault location scheme for low voltage smart distribution systems

Salar Naderi,[1] Abbas Ketabi,[1] and Iman Sadeghkhani[2,3,✉]

[1]*Department of Electrical and Computer Engineering, University of Kashan, Kashan, Iran*

[2]*Smart Microgrid Research Center, Najafabad Branch, Islamic Azad University, Najafabad, Iran*

[3]*Department of Electrical Engineering, Najafabad Branch, Islamic Azad University, Najafabad, Iran*

✉ E-mail: sadeghkhani@pel.iaun.ac.ir

Integrating the self-healing capability realizes the automated protection of smart distribution systems. This article presents a fault location scheme for low voltage (LV) distribution systems based on the information collected from the smart meters. First, a fault condition is detected and classified by processing the current signal at the secondary side of the distribution transformer by an intelligent electronic device. Then, the faulty feeder and section are determined by calculating the fault-imposed component of nodal voltages. The reliable performance of the proposed scheme is verified through several case studies using a real semi-rural distribution system.

Introduction: Distribution systems are vulnerable to various faults, such as short circuits, overloads, and equipment failures, which can disrupt the power supply and pose significant risks to equipment and personnel. Thus, the protection of distribution systems is a critical aspect of ensuring the safe and reliable delivery of electricity to consumers. Traditionally, current-based protective devices such as overcurrent relays and fuses detect abnormal conditions and quickly isolate the faulty area to limit the fault impact and minimize downtime. However, locating the faults is a challenging task as they are located without any measurement, for example, by using the fuse and fault locator operation or relay targets [1]. It increases the average duration of interruptions experienced by customers served by the distribution system. According to the U.S. energy information administration report, the system average interruption duration index (SAIDI) for the U.S. distribution system in 2021 will be 475.8 and 125.7 min with and without considering major event days, respectively [2].

To improve the SAIDI, several fault location schemes are proposed in the literature [3, 4]. However, the vast majority of these schemes are presented for medium voltage (MV) distribution systems, and less attention is paid by researchers to developing fault location schemes for low voltage (LV) distribution systems with more complex structures and lower measurements. The complexity is due to the integration of single-phase loads and residential photovoltaic (PV) systems (imbalance), the presence of different types of conductors (heterogeneity), and the increased number of branches. These features degrade the performance of some MV fault location schemes; for example, the calculated distance by the impedance-based methods may determine multiple possible fault locations.

The fault location process of LV grids in many utilities is still based on customer phone calls. To automate this process, a few schemes are presented that can be categorized into three groups: i) learning-based, ii) reflectometry-based and iii) sparse measurements-based schemes. The first group of schemes use a learning method including gradient boosting trees [5], extreme gradient boosting [6], deep neural networks [7], and similarity criteria in the principal component subspace [8]. However, they suffer from the need for a training dataset. The second group schemes consist of injecting a high-frequency component and logging the line response [9], intelligent processing of time domain reflectometry by using very high sampling frequency equipment [10], and chaotic reflection measurement [11]. However, the performance of reflectometry-based schemes may determine multiple fault locations with an increased number of branches. The third group schemes use distributed measurements to locate a fault condition. In [12], current measurement units are installed at the head end of each branch to determine the amplitude and direction of the fault current. The current angle difference in two ends of feeder sections is the basis of the scheme presented in [13]. However, these schemes suffer from the need for current phasor measurement units (PMUs) that are not available in the LV distribution systems. With emerging smart distribution systems, advanced sensing, communication, and control technologies are integrated to enhance grid intelligence, flexibility, and reliability. The key components of smart grids such as smart meters, advanced sensors, and automation systems enable monitoring and data-driven decision-making, aiding to self-heal the smart distribution systems after the fault occurrence. By analyzing the voltage amplitude measurement by smart meters installed in feeder nodes, [14, 15] locate the fault. However, they suffer from disability in locating a fault in the first and last sectors of a feeder. Initiated by a customer phone call, a fault is located in [16] by using the status of receiving data from smart meters. However, it suffers from accurate faulty section identification in complex distribution systems and longer downtime due to dependency on customer phone calls. Moreover, except for the scheme in [13], none of the schemes of the three groups consider double-line and double-line to ground faults.

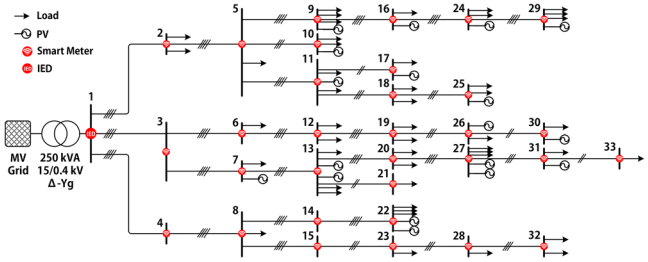

Fig. 1 *Singe-line diagram of the study low voltage smart distribution system*

To address the limitations of third group schemes including the need for PMU, the inability to locate a fault in all sections of the feeder, the inability to locate a fault in a complex grid, and no evaluation for all types of fault, this article presents a fault location scheme for LV smart distribution systems based on the collected data from smart meters. In the first step, a fault condition is detected and classified based on the fault-imposed component of the secondary side current of the distribution transformer by an intelligent electronic device (IED). Then, the IED processes the collected voltage measurements from smart meters to determine the faulty feeder and section. The proposed fault location technique is based on the fault-imposed component of nodal voltages.

Proposed scheme: Figure 1 shows the single-line diagram of the study test system, which is a semi-rural three-phase four-wire LV distribution system [17]. It consists of three feeders and 33 nodes and includes three-phase, two-phase, and single-phase lines with various cable types and lengths. To capture the benefits of PV systems [18, 19], 18 single-phase residential PV units are integrated into the study system. These PV units, as well as 48 single-phase loads, are unsymmetrically distributed along the feeders. The study smart test system is equipped with 32 single- and multi-phase smart meters at all nodes for voltage measurement and one IED at the root node (node 1) for current measurement and data processing. The use of IED reduces the computational burden of the distribution system control center.

Fault detection and classification: A fault condition is detected by the IED. It monitors the symmetrical components of node 1 current which are calculated as

$$\begin{bmatrix} I_{p1}^{\text{pu}} \\ I_{n1}^{\text{pu}} \\ I_{z1}^{\text{pu}} \end{bmatrix} = \frac{1}{3} \begin{bmatrix} 1 & \alpha & \alpha^2 \\ 1 & \alpha^2 & \alpha \\ 1 & 1 & 1 \end{bmatrix} \begin{bmatrix} I_{a1} \\ I_{b1} \\ I_{c1} \end{bmatrix} \times \frac{1}{I_{\text{base}}} \tag{1}$$

where I_{p1}, I_{n1}, and I_{z1} are the normalized positive-sequence, negative-sequence, and zero-sequence components of node 1 current, respectively. I_{a1}, I_{b1}, and I_{c1} are the phase current measurements at node 1, and $\alpha = 1\angle 120^\circ$. I_{base} is the base current for normalization and is calculated as $I_{\text{base}} = S_{\text{base}}/V_{\text{base}}$, where S_{base} and V_{base} are the base power and voltage and are chosen to be 250 kVA and $400/\sqrt{3}$ V, respectively. Then,

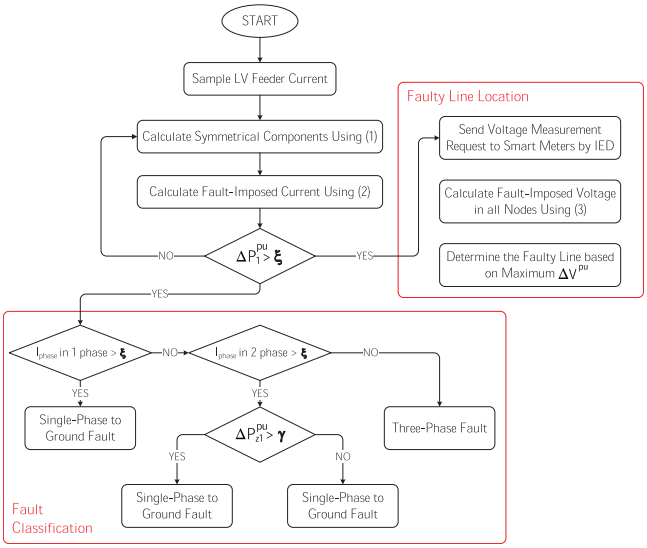

Fig. 2 *Flowchart of the proposed protection scheme*

the fault-imposed components of current symmetrical components are calculated by using the Delta filter [20] as

$$\Delta I^{\mathrm{pu}}[k] = \left| I^{\mathrm{pu}}[k] - I^{\mathrm{pu}}[k - k_d] \right|, \tag{2}$$

where k_d is the number of time delay samples of the Delta filter. The fault-imposed component is near zero during normal operation, while it changes to a non-zero value during a fault condition. Also, it reduces the impact of the presence of zero-sequence current in normal operating conditions due to the inherent imbalance of LV systems on the performance of fault classification in the next step. A fault condition is verified if $\Delta I_{p1}^{\mathrm{pu}} > \xi$, where ξ is the fault detection threshold.

To classify the fault, the phase current measurements are monitored. If the amplitude of the current in all phases increases, the fault is classified as a three-phase fault. If the amplitude of the current in one phase increases, it is classified as a single-phase-to-ground fault. In the case of increasing the amplitude of current in two phases, the fault-imposed component of zero-sequence current is monitored. A fault is classified as a double-line to ground fault if $\Delta I_{z1}^{\mathrm{pu}} > \gamma$, where γ is the double-line classification threshold. Otherwise, it is classified as a double-line fault.

Fault location: In normal operating conditions, the smart meters periodically send their voltage amplitudes to the IED. Although they are capable of providing this measurement every 1 to 10 s, the communication limitations decrease this measurement frequency to 15 min [7]. When a fault condition is verified, the IED sends a request to all smart meters to send their voltage measurements. The node with the lowest voltage amplitude is not necessarily the faulty node. To address this issue, this article presents a fault location index (FLI) based on the fault-imposed components of nodal voltages as

$$\mathrm{FLI}_i = \left| \Delta V_i^{\mathrm{pu}}[k] \right| = \left| V_i^{\mathrm{pu}}[k] - V_i^{\mathrm{pu}}[k-1] \right|, \tag{3}$$

where FLI_i is the fault location index in node i and ΔV_i^{pu} is the fault-imposed component of normalized voltage in node i. When a fault occurs in a certain section, the faulty node has the highest voltage change with respect to the normal condition, as after the fault location, there is no significant voltage support due to the radial structure; thus, closer to the fault location, the higher ΔV^{pu}. By comparing the collected nodal voltages during the fault condition with the previous collected nodal voltages during normal operation, the IED finds the faulty node: ΔV^{pu} is calculated for all nodes; the section before the node with the highest FLI is determined as the faulty section. Figure 2 shows the flowchart of the proposed protection scheme for LV grids.

It should be noted that according to the International Renewable Energy Agency (IRENA) grid code for renewable-powered systems [21], the low-voltage ride through (LVRT) capability is now required for distributed energy resources connected to low-voltage distribution systems to improve system reliability. However, there is no requirement for voltage support by injecting reactive power during LVRT events.

In addition, according to the EN 50160 standard [22], the permissible voltage drop in LV grids is 10% of the nominal voltage. It means that by using the limited measurement capability of available commercial smart meters, that is, voltage magnitude reports every 15 min, the detection of high-impedance faults (HIFs) is not possible as the voltage magnitude is inside the permissible range. However, since an IED is installed at the secondary side of the distribution transformer, an available HIF detection method such as those proposed in [23] can be integrated into the proposed scheme. Nevertheless, the detection of HIFs is out of the scope of this article.

Table 1. Fault-imposed components during an a–b *fault at sections 13–20*

ΔI_{p1}^{pu}	$\Delta I_{n1}^{\mathbf{pu}}$	ΔI_{z1}^{pu}	ΔI_{a1}^{pu}	ΔI_{b1}^{pu}	ΔI_{c1}^{pu}
1.0509	0.8709	0.0006	1.2254	1.1955	0.0290
Fault location index in phase B (pu)					
Feeder 1		**Feeder 2**		**Feeder 3**	
SM2	0.2135	SM3	0.2785	SM4	0.2201
SM5	0.2094	SM6	0.2741	SM8	0.2179
SM9	0.2069	SM12	0.2594	SM15	0.2152
SM16	0.2058	SM19	0.2578	SM23	0.2093
SM24	0.2047	SM26	0.257	SM28	0.1899
SM29	0.2031	SM30	—	SM32	0.1877
SM10	0.2049	SM7	0.4532	SM14	0.2161
SM11	0.2056	SM13	0.4939	SM22	0.2054
SM17	—	SM20	0.5023		
SM18	0.204	SM27	0.5002		
SM25	0.2026	SM31	0.4927		
		SM33	—		
		SM21	0.4763		

Abbreviations: PMU, phasor measurement unit; SM, smart meter.

Performance evaluation: To evaluate the performance of the proposed scheme, the study test system in Figure 1 is simulated in the MATLAB/Simulink environment. Several single- and multi-phase fault scenarios at different points of the feeder with various fault resistances and several no-fault scenarios including large load and PV switchings are conducted to determine thresholds of fault detection ξ and double-line classification γ; they are chosen to be 0.11 and 0.015 pu, respectively. The fault-imposed components should be calculated at the early stages of semi-steady-state conditions during the fault but before any operation of protective devices; in this article, the calculations are performed 150 ms after the fault occurrence [14]. Regarding the sampling frequency of 1 kHz of the IED, k_d is chosen to be 150 samples. In the first case study, a solid double-line (a-b) fault occurs at sections 13–20 (the section between nodes 13 and 20) as a fault in the middle of a feeder. Table 1 presents the fault-imposed components of sequence and phase components of node 1 current as well as fault-imposed nodal voltages at phase b. The "—" line represents the lack of a smart meter at phase b in that node due to the absence of one (two) phase(s). $\Delta I_{p1}^{\mathrm{pu}}$ exceed ξ and the fault is detected. Since only fault-imposed components of phases a and b exceed the threshold and there is no fault-imposed zero-sequence component, the fault is correctly classified as an a–b fault. Then, the IED processes the collected data from smart meters. The voltage magnitude of the smart meter at node 20 (SM20) has the highest ΔV^{pu}. Thus, sections 13–20 are correctly determined to be the faulty section.

In the next case study, a single-phase to ground fault (c-g) with a fault resistance of 1 Ω is simulated at sections 18–25 as a fault in the last section of a feeder. As presented in Table 2, the fault is correctly

Table 2. Fault-imposed components during a c–g fault at sections 18–25

ΔI_{p1}^{pu}	ΔI_{n1}^{pu}	ΔI_{z1}^{pu}	ΔI_{a1}^{pu}	ΔI_{b1}^{pu}	ΔI_{c1}^{pu}
0.1424	0.0339	0.0838	0.0418	0.0503	0.2048
Fault location index in phase C (pu)					
Feeder 1		Feeder 2		Feeder 3	
SM2	0.0306	SM3	0.0056	SM4	0.0026
SM5	0.046	SM6	0.0058	SM8	0.0029
SM9	0.0458	SM12	0.0065	SM15	0.0031
SM16	0.0457	SM19	0.0066	SM23	0.0036
SM24	0.0455	SM26	0.0066	SM28	0.0045
SM29	0.0451	SM30	0.0068	SM32	0.0048
SM10	—	SM7	0.0174	SM14	0.003
SM11	0.1588	SM13	0.0214	SM22	0.0039
SM17	—	SM20	0.0472		
SM18	0.2092	SM27	0.0629		
SM25	0.2503	SM31	0.0625		
		SM33	0.0623		
		SM21	—		

Abbreviations: PMU, phasor measurement unit; SM, smart meter.

Table 3. Fault-imposed components during a three-phase fault at sections 1–4

ΔI_{p1}^{pu}	ΔI_{n1}^{pu}	ΔI_{z1}^{pu}	ΔI_{a1}^{pu}	$\Delta I_{\mathbf{b1}}^{pu}$	ΔI_{c1}^{pu}
5.3745	0.0845	0.0091	3.8670	3.7697	3.7578
Fault location index in phase A (pu)					
Feeder 1		**Feeder 2**		**Feeder 3**	
SM2	0.6389	SM3	0.6496	SM4	0.8541
SM5	0.6311	SM6	0.6418	SM8	0.8516
SM9	0.6266	SM12	0.624	SM15	—
SM16	0.6259	SM19	0.6227	SM23	—
SM24	0.6245	SM26	—	SM28	—
SM29	0.6192	SM30	—	SM32	—
SM10	0.628	SM7	0.6384	SM14	0.8324
SM11	0.6074	SM13	0.6369	SM22	0.7191
SM17	0.5879	SM20	0.637		
SM18	—	SM27	0.6317		
SM25	—	SM31	0		
		SM33	—		
		SM21	—		

Abbreviations: PMU, phasor measurement unit; SM, smart meter.

detected as a *c-g* fault as only ΔI_{c1}^{pu} exceeds the threshold. In addition, the voltage reported by SM25 has the highest change with respect to normal operation. Thus, sections 18–25 are determined as the faulty section.

Depending on the class, the accuracy of smart meters is within ±0.2% or ±0.5% [24]. A solid three-phase fault is simulated at sections 1–4 as the first section of a feeder while the smart meter of node 2 as the faulty node has a −0.5% error. Table 3 presents the results. The real ΔV_{a4}^{pu} is 0.8584 pu which is reduced to 0.8541 pu due to the measurement error. Nevertheless, the faulty section is correctly determined as sections 1–4.

To evaluate the performance of the proposed scheme in the case of information loss, a double-line to ground (*b-c-g*) fault at sections 19–26 with fault resistance of 5 Ω is simulated while the data of node 26

Table 4. Fault-imposed components during a b–c–g fault at sections 19–26

ΔI_{p1}^{pu}	ΔI_{n1}^{pu}	ΔI_{z1}^{pu}	ΔI_{a1}^{pu}	ΔI_{b1}^{pu}	ΔI_{c1}^{pu}
0.1162	0.0228	0.0270	0.0472	0.1045	0.0937
Fault location index in phase B (pu)					
Feeder 1		**Feeder 2**		**Feeder 3**	
SM2	0.0017	SM3	0.0075	SM4	0.0017
SM5	0.0017	SM6	0.019	SM8	0.0017
SM9	0.0018	SM12	0.0634	SM15	0.0017
SM16	0.0018	SM19	0.0693	SM23	0.0018
SM24	0.0018	SM26	LOST	SM28	0.002
SM29	0.0018	SM30	—	SM32	0.0021
SM10	0.0017	SM7	0.0186	SM14	0.0017
SM11	0.0018	SM13	0.0223	SM22	0.0019
SM17	—	SM20	0.0471		
SM18	0.0018	SM27	0.0618		
SM25	0.0018	SM31	0.0607		
		SM33	—		
		SM21	0.0216		

Abbreviations: PMU, phasor measurement unit; SM, smart meter.

Table 5. Comparison of the proposed scheme with sparse measurements-based schemes

	[12]	[13]	[14]	[15]	[16]	Proposed scheme
Does the scheme require no PMU?	✗	✗	✓	✓	✓	✓
Is the scheme able to locate a fault in all feeder sectors?	✓	✓	✗	✗	✓	✓
Can the scheme be used in a complex grid?	✓	✓	✓	✓	✗	✓
Is the scheme evaluated for all types of faults?	✗	✓	✗	✗	✗	✓

is not received by the IED due to smart meter/communication failure. As presented in Table 4, the fault-imposed voltage of node 19 has the highest value, and the fault is located between nodes 12 and 19. Thus, the information loss results in one section error in locating the fault in this case. Moreover, the fault is classified as a double-line to ground fault as the zero-sequence current exceeds the double-line classification threshold γ.

Table 5 compares the features of the proposed fault location scheme with other sparse measurement-based schemes. Unlike [14, 15], the proposed scheme can locate a fault condition in the first and last sections of a feeder. Also, unlike [16], the proposed scheme can locate the faulty section in a complex distribution system. Moreover, unlike [12, 13], the proposed scheme does not require PMU. In addition, unlike most of these references, the performance of the proposed scheme is evaluated for all types of fault.

Conclusion: Based on the available voltage measurement by smart meters, this article presents a fault location scheme for a smart LV distribution system. The faulty feeder and section are located by calculating the fault-imposed component of nodal voltages using an IED installed at the root node of the grid. The IED also detects and classifies the fault by processing the current signal of the root node. The proposed scheme can locate all types of faults in all sections of a feeder, even in a complex distribution system, and without the need for the PMU. Several single- and multi-phase fault scenarios in an unbalanced heterogeneous distribution system demonstrate the proper performance of the proposed scheme even in the presence of measurement error up to 0.5% and information

loss. Determination of faulty points along the section, accurate faulty section location in the case of information loss or a limited number of smart meters, and locating simultaneous faults and HIFs can be considered as the next step of this work.

Conflict of interest statement: The authors declare that there is no conflicts of interest.

Author contributions: **Salar Naderi**: Investigation; software; writing—original draft. **Abbas Ketabi**: Conceptualization; supervision; writing—review and editing. **Iman Sadeghkhani**: Conceptualization; methodology; supervision; visualization; writing—original draft.

Data availability statement: Data sharing is not applicable to this article as no new data were created or analyzed in this study.

Received: *4 August 2023* Accepted: *6 December 2023*
doi: 10.1049/ell2.13062

References

1 Trindade, F.C.L., Freitas, W.: Low voltage zones to support fault location in distribution systems with smart meters. *IEEE Trans. Smart Grid* **8**(6), 2765–2774 (2017)
2 Electric power annual 2021. U.S. Energy Information Administration Washington, DC (2022)
3 Bahmanyar, A., Jamali, S., Estebsari, A., Bompard, E.: A comparison framework for distribution system outage and fault location methods. *Electr. Power Syst. Res.* **145**, 19–34 (2017)
4 Stefanidou-Voziki, P., Sapountzoglou, N., Raison, B., Dominguez-Garcia, J.L.: A review of fault location and classification methods in distribution grids. *Electr. Power Syst. Res.* **209**, 108031 (2022)
5 Sapountzoglou, N., Lago, J., Raison, B.: Fault diagnosis in low voltage smart distribution grids using gradient boosting trees. *Electr. Power Syst. Res.* **182**, 106254 (2020)
6 Stefanidou-Voziki, P., Cardoner-Valbuena, D., Villafafila-Robles, R., Dominguez-Garcia, J.L.: Data analysis and management for optimal application of an advanced ML-based fault location algorithm for low voltage grids. *Int. J. Electr. Power Energy Syst.* **142**, 108303 (2022)
7 Sapountzoglou, N., Lago, J., De Schutter, B., Raison, B.: A generalizable and sensor-independent deep learning method for fault detection and location in low-voltage distribution grids. *Appl. Energy* **276**, 115299 (2020)
8 Souto, L., Meléndez, J., Herraiz, S.: Fault location in low voltage smart grids based on similarity criteria in the principal component subspace. In: Proceedings of IEEE Power & Energy Society Innovative Smart Grid Technologies Conference (ISGT), pp. 1–5. IEEE, Piscataway, NJ (2020)
9 Ballestín-Fuertes, J., Cervero, D., Bludszuweit, H., Martínez, R., Castro, J.A.S.: Fault location in low-voltage distribution networks based on reflectometry—A case study. *Renewable Energy Power Qual. J.* **18**, 735–740 (2020)
10 Siew, W., Soraghan, J., Stewart, M., Fisher, D., Fraser, D., Asif, M.: Intelligent fault location for low voltage distribution networks. Presented at the CIRED 19th International Conference on Electricity Distribution, Vienna, 21–24 May 2007
11 Li, S., Zeng, Y.: Research on fault location of distributed low-voltage distribution network based on internet of things. In: International Conference on Computer Network, Electronic and Automation (ICCNEA), pp. 258–262. IEEE, Piscataway, NJ (2021)
12 Yang, F., Zhixiang, Z., Zha, X., Jian, L., Jianyong, C.: Low-voltage active distribution network fault location system considering information distortion. In: International Conference on Manufacturing, Industrial Automation and Electronics (ICMIAE), pp. 335–338. IEEE, Piscataway, NJ (2022)
13 Niu, G., Zhou, L., Pei, W., Qi, Z.: {\it A novel fault location and recognition method for low voltage active distribution network}. In: 5th International Conference on Electric Utility Deregulation and Restructuring and Power Technologies (DRPT), pp. 876–881. IEEE, Piscataway, NJ (2015)
14 Sapountzoglou, N., Raison, B., Silva, N.: A fault localization method for single-phase to ground faults in LV smart distribution grids. In: Zamboni, W., Petrone, G., (eds.) Electrimas 2019, pp. 327–338. Springer International Publishing, Cham (2020)
15 Sapountzoglou, N., Raison, B., Silva, N.: Fault detection and localization in LV smart grids. In: 2019 Milan PowerTech, pp. 1–6. IEEE, Piscataway, NJ (2019)
16 Sun, K., Chen, Q., Gao, Z.: An automatic faulted line section location method for electric power distribution systems based on multisource information. *IEEE Trans. Power Delivery* **31**(4), 1542–1551 (2016)
17 Sapountzoglou, N.: Fault detection and isolation for low voltage distribution grids with distributed generation. Université Grenoble Alpes, Saint-Martin-d'Hères, France (2019)
18 Khoshnami, A., Sadeghkhani, I.: Fault detection for PV systems using Teager–Kaiser energy operator. *Electron. Lett.* **54**(23), 1342–1344 (2018)
19 Zhang, Z., Dou, C., Yue, D., Zhang, B.: High-accuracy voltage regulation method for PV distribution systems. *Electron. Lett.* **55**(10), 615–617 (2019)
20 Benmouy, G., Roberts, J.: Superimposed quantities: Their true nature and application in relays. In: 26th Annual Western Protective Relay Conference. Spokane, Washington (1999)
21 Agency, I.R.E.: Grid codes for renewable powered systems. International Renewable Energy Agency Abu Dhabi, United Arab Emirates (2022)
22 Markiewicz, H., Klajn, A.: Power quality application guide: Standard EN 50160 - Voltage characteristics in public distribution systems (2004)
23 Nezamzadeh-Ejieh, S., Sadeghkhani, I.: HIF detection in distribution networks based on Kullback-Leibler divergence. *IET Gener. Transm. Distrib.* **14**(1), 29–36 (2020)
24 Chakraborty, S., Das, S., Sidhu, T., Siva, A.K.: Smart meters for enhancing protection and monitoring functions in emerging distribution systems. *Int. J. Electr. Power Energy Syst.* **127**, 106626 (2021)